International Colloquium on Jets, Wakes and Shear Layers
Melbourne, Australia, 18–20 April 1994

THREE-DIMENSIONAL INSTABILITIES IN THE WAKE OF A CIRCULAR CYLINDER

Mark Thompson and Kerry Hourigan
CSIRO Division of Building, Construction and Engineering,
P.O. Box 56, Highett, Victoria, 3190, AUSTRALIA
and
John Sheridan
Department of Mechanical Engineering, Monash University,
Clayton, Victoria, 3190, AUSTRALIA

ABSTRACT

The three-dimensional wake structure behind a circular cylinder has been computed using a high-order spectral-element technique. The two modes of three-dimensional instability, designated as Modes A and B, both found experimentally but not previously computationally, have been captured. Mode A appears first at a Reynolds number slightly less than 200. As the Reynolds number is increased there is a transfer of energy to Mode B which has a wavelength approximately one quarter of that of Mode A.

INTRODUCTION

Despite the fact that the flow past a circular cylinder has been studied for well over one hundred years, and that the geometrical configuration is a particularly simple one, this problem is still under intensive investigation today. Indeed within the last ten years, due to the efforts of many research groups (Williamson 1988b 1991a 1991b, Hamache and Gharib 1989, Norberg 1994, Eisenlohr and Eckelmann 1989), the experimental relationship between Strouhal and Reynolds number has been now determined to within one percent, at least within the two-dimensional shedding regime. The previous discrepancies between different experimental teams seem to have stemmed from various factors including small aspect ratio cylinders, end effects and oblique modes. The new "universal" results represent a challenge for computationalists who in the past have relied on the variation in the experimental results to justify their predictions.

At a Reynolds number of approximately 180, the two-dimensional periodic Strouhal vortex wake undergoes a transition to three-dimensionality. This was observed by (Roshko 1954, 1955) in the form of irregularities in the wake velocity fluctuations. Recent experiments undertaken by Williamson (1988b) have demonstrated that the transition to three-dimensionality involves two modes of formation of streamwise vorticity in the near wake. The two modes are dominant over different Reynolds number ranges.

When the wake first becomes three-dimensional, at $Re \approx 180$ ($Re = u_\infty D/\nu$, where ν is the kinematic viscosity, D is the cylinder diameter and u_∞ is the freestream velocity), Mode A vortex shedding appears. This is characterised by regular streamwise vortices appearing in the wake, with a spanwise wavelength of approximately 3 cylinder diameters. At $Re \approx 230$, a second mode (Mode B) appears, consisting of a more irregular array of streamwise vortices with a mean spanwise wavelength of about 1 cylinder diameter. Between $Re = 230$ and

$Re = 260$, there is a steady transfer of energy from Mode A to Mode B. At each of these transitions, a discontinuity in the Strouhal number versus Reynolds number curve occurs. The appearance of Mode A is hysteretic, while that of Mode B is not.

Until recently there have been few numerical studies published on the three-dimensional wakes due to the significant computational resources required to properly resolve the flow structures. One investigation undertaken by Karniadakis and Triantafyllou (1992) concentrated on the stability of the wake of a circular cylinder over a Reynolds number range up to 500, rather than a detailed study of the different modes that appear. The emphasis was on examining the route to fully turbulent flow followed by this (and similar) flows. Computational restrictions led them to use a fairly coarse mesh with a spanwise domain size that was too short to capture Mode A. They suggest that the route to wake turbulence is via period-doubling.

In this paper, some preliminary results from numerical experiments examining both two- and three-dimensional flows are presented. The results of the simulations are compared with experimental results.

PROBLEM FORMULATION AND NUMERICAL METHODS

The governing equations are the incompressible time-dependent Navier-Stokes equations in primitive variable form. The equations are discretised using a time-split spectral/spectral-element method as described by Karniadakis and Triantafyllou (1992) and Tomboulides *et al.* (1992) and references cited therein. Consequently only a brief overview will be presented here.

Time-Stepping Scheme

The momentum equations are integrated forward in time by a three-step procedure. The steps account for the convection, pressure and diffusion terms respectively. The equation treating the convection term is treated explicitly because of its nonlinear nature. The equations for the diffusion and the pressure are treated implicitly. If memory is available the matrices involved can be inverted in a preprocessing step. Otherwise, efficient iterative techniques for symmetric problems can be used (*i.e.*, conjugate gradient methods). For the calculations described in this paper only direct solvers were used.

The convection equation is integrated forward in time by the third-order Adams-Bashforth method and the diffusion equation is treated by the Crank-Nicholson scheme. In the second step, the pressure is evaluated. A Poisson equation is formed by taking the divergence of the equation for the pressure substep and continuity is enforced at the end of the substep. Second-order overall time accuracy is achieved by using a higher-order pressure boundary condition as described in Karniadakis *et al.* (1991).

Spatial Discretisation

The spectral-element technique (Karniadakis and Triantafyllou 1992) is employed for the two-dimensional (streamwise) flow (*i.e.*, the x-y planes). A typical (two-dimensional) spectral-element mesh is shown in Fig. 1. It consists of a $K = 60$ macro elements. Each element is mapped into a computational square and high-order Lagrangian polynomial interpolants are used to approximate the solution variables in each direction. The Galerkin finite-element method is applied to form equations for the solution variables at the nodal points. The integrals of the flow equations multiplied by the local weighting functions are (approximately) evaluated by Gauss-Legendre-Lobatto quadrature. This approach is particularly economical

computationally in that only a limited number of element nodes contribute to the equations formed at a particular node. For example, the "Mass" matrix is diagonal in this case; this would not occur if Gauss-Legendre quadrature was used, for example. Further economy is gained by using static-condensation techniques. This method relies on the fact that the equations for the internal nodes of each element only depend on the boundary nodes, and hence the matrix equations can be decoupled into two sets; one involving the element boundary nodes, and K small matrix equations for the internal nodes of each element. The latter K equations can be evaluated after the first (larger) matrix equation is solved. Bandwidth minimisation scheme can reduce the bandwidth (and hopefully overall size) of the matrices and sparse matrix solvers are used to solve the large systems of equations involved. Due to the form of the splitting scheme the matrix inversions only need to be performed at the beginning of the calculations.

A Fourier spectral discretisation is employed in the spanwise direction. This has significant computational benefits. The equations for each Fourier mode decouple, leading to small matrix equations for each mode rather than a large coupled matrix equation with a large bandwidth that would be much more computationally expensive. An efficient implementation can be achieved on parallel architecture machines due (in part) to this decoupling. For the work described here, though, the computations were performed in double precision on a serial Silicon Graphics workstation rated at about 12 Megaflops with 12 Megawords of main memory.

TWO-DIMENSIONAL STUDIES

As mentioned previously, experimental studies indicate the wake becomes three-dimensional at a Reynolds number around 180. Two-dimensional simulations below this Reynolds number should adequately reproduce the results of experimental measurements which are believed to be within 1% for the Strouhal number (Williamson 1991a). At higher Reynolds numbers, two-dimensional computations can provide a comparison for three-dimensional computations and experiments.

Strouhal Number

In previous computational studies, an often-quoted test of accuracy for cylinder flow computations has been the variation of Strouhal number with Reynolds number. Williamson (1991a) has given a least-squares fit to the universal Strouhal number curve for the low Reynolds number regime as

$$St = \frac{A}{Re} + B + C\ Re, \tag{1}$$

where $A = -3.3265$, $B = 0.1816$ and $C = 0.00016$.

The three-dimensional computations require a considerable amount of CPU time and memory and hence for this preliminary study at least, the three-dimensional runs were done on a *small* mesh. The aim of this section is to verify that the computational scheme can reproduce two-dimensional experimental results to within experimental error and to establish the effect of using a domain smaller than desirable.

Karniadakis and Triantafyllou (1992) found in their numerical experiments that, over a limited number of tests, the Strouhal number (a) increased with decreasing inflow length, (b) was insensitive to the outflow length (between 36 and 70 cylinder radii), (c) increased with decreasing domain width. They also confirmed that the level of resolution that they used was sufficient by showing that increasing the resolution per element did not affect the Strouhal number.

Table 1: Dependence of Strouhal number on polynomial order for small mesh at Re = 200 for a constant timestep of 0.01. (Two-dimensional simulation)

Element size ($N \times N$)	Strouhal Number
5×5	0.2036
7×7	0.2101
9×9	0.2107
11×11	0.2107
13×13	0.2108

The domain is described by three main parameters: the number of elements (K), and inflow length and domain width (X_i) and the outflow length (X_o). In addition, the distribution of elements within the domain also will strongly influence the overall accuracy of the results. The mesh used for the three-dimensional calculations is shown in Fig. 1. This has $X_i = 7R$ and $X_o = 24.5R$. Some larger meshes were used to try to reproduce the two-dimensional results as accurately as possible. They used this mesh as a basis together with either or both of (a) an *expandable* layer of elements to extend the inflow length and domain width and (b) elements extending the outflow length.

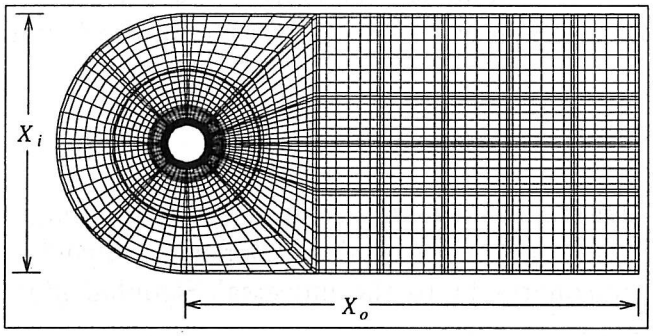

Figure 1: Left: Two-dimensional view of three-dimensional mesh system showing the spectral element discretisation. This mesh has $K = 60$ elements.

The effect of the number of nodes per element in each direction (N) is shown in Table (1). (Note that the order is the interpolating polynomial is $N - 1$.) For a calculation at $Re = 200$ on the mesh shown in Fig. 1 the Strouhal number has converged to better than 0.1% by $N = 9$.

The Strouhal number is sensitive to the size of the domain. An accurate determination (to within the error in the experimental values) requires the outer boundary to be placed approximately $50R$ from the cylinder. The inflow and outer boundary conditions will obviously affect this conclusion. For the present computations, the inflow and outer boundary conditions are taken from the potential flow solution. Also, the outflow boundary conditions

are taken to be $\partial \mathbf{v}/\partial n = 0$ and $p = 0$. For all these runs the shedding becomes truly periodic at the Strouhal frequency with no other identifiable frequency components.

Figure 2 shows computations of the St–Re relationship for two different mesh systems: the mesh shown in Fig. 1 (round symbols) and a mesh corresponding a larger domain ($X_i = 50D$, $K = 106$, $X_o = 42.5R$) (square symbols). Each mesh has 9×9 nodes per element. The curve of best fit to the experimental data, given by equation (1), is shown for comparison. The results for the large domain are within 1% of the experimental values for the two-dimensional shedding range. For the smaller mesh, the results are within about 7%. It is believed that the restricted domain should not alter the essential physics underlying the development and interaction of the three-dimensional structures although it might influence variables such as the Reynolds number at which three-dimensionality first occurs.

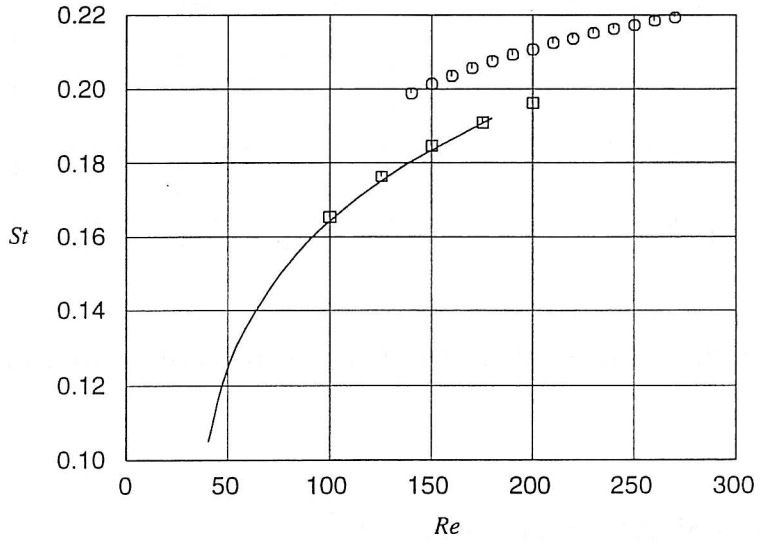

Figure 2: Variation of Strouhal number with Reynolds number. The square symbols indicate results for large domain (106 9×9 elements, $X_i = 50D$, $X_o = 42.5R$) and the rounded symbols are for the small mesh used for the 3D calculations (60 9×9) elements. The solid curve shows the experimental result (Williamson 1991a).

Other Tests

Although spectral-element/spectral methods possess the property of *exponential* convergence (*i.e.*, converging faster than any power of the number of nodes), in practice, this asymptotic convergence rate may have little relevance. Unless the number of nodes per element is large enough so that flow features can be resolved by the functional representation, these methods can be worse than using much lower-order methods. A recent case in point is Kaiktsis *et al.* (1993). This paper presents results for flow past a backward-facing step and predicts unsteady behaviour at $Re = 800$. This prediction appears to be a result of inadequate resolution. Most other computations using different methods indicate the flow is steady and importantly calculations using a very similar spectral-element code with more nodes per element also indicate a steady flow (Gresho *et al* 1993).

The Strouhal number may not be a very sensitive indicator that a particular mesh system has sufficient resolution to adequately resolve the flow field. It may, for instance, depend more on the grid resolution in the neighbourhood of the cylinder and not the downstream

resolution. An alternative test is to look at the variation of the velocity field at a point some distance downstream of the cylinder. Figure 3 shows the dependence of the extremes of the u component of the velocity against the element order N. These values are taken at a point $7R$ downstream of the cylinder at $Re = 200$. Clearly, the curves are beginning to flatten out at $N = 9$.

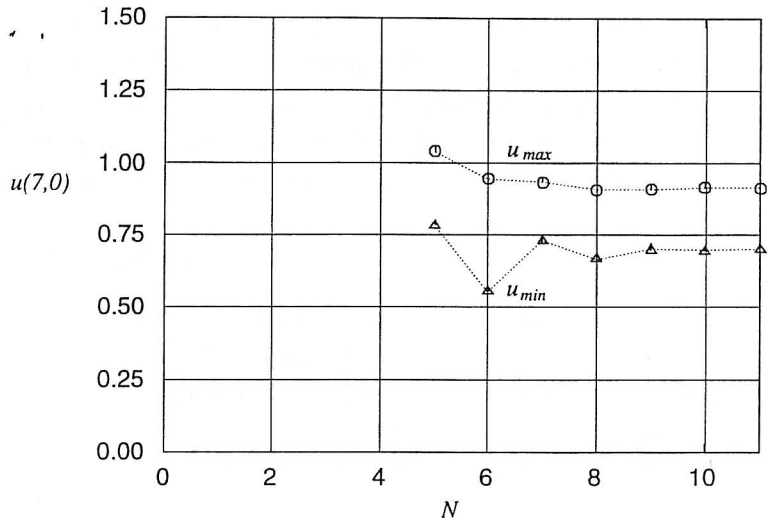

Figure 3: Dependence of the extremes of $u(7, 0)$ on polynomial order N for mesh A at $Re = 200$.

THREE-DIMENSIONAL SIMULATIONS

Numerical simulations of the onset of three-dimensionality have been reported previously by Karniadakis and Triantafyllou (1992) and Tomboulides *et al.* (1992). In their studies, emphasis was placed on the stability analysis and transition to turbulence. In the current study, the focus is on the appearance of the two three-dimensional instability modes, A and B, and the transfer of energy between the two modes as the Reynolds number is increased. The topology of the three-dimensional structures is also examined.

Simulation at $Re = 250$

To investigate the development of the three-dimensional instability a computation was performed at $Re = 250$, with 24 Fourier modes and a spanwise periodicity length of πD. This domain width was chosen from the observations of Williamson (1988b) who observed the spanwise wavelength for Mode A to be approximately $3D$. The computation was started from the periodic field taken from a two-dimensional simulation. The initially zero w velocity component was perturbed by a random amount at each point (at a level of 10^{-4}) to accelerate development of the three-dimensionality. After six Strouhal shedding cycles plots of isosurfaces of the streamwise vorticity clearly show the appearance of coherent three-dimensional structures with a spanwise wavelength of πD. The magnitude of the streamwise vorticity is very low at this time. The maximum value over the field is about 0.02. After fifteen cycles, the structures are much stronger still with a wavelength of $3D$. At 25 cycles, the structures have almost reached maximum strength ($\max(\omega_{st} \equiv \sqrt{\omega_x^2 + \omega_y^2}) \approx 3$). There also appears to be some finer scale structure developing at this time.

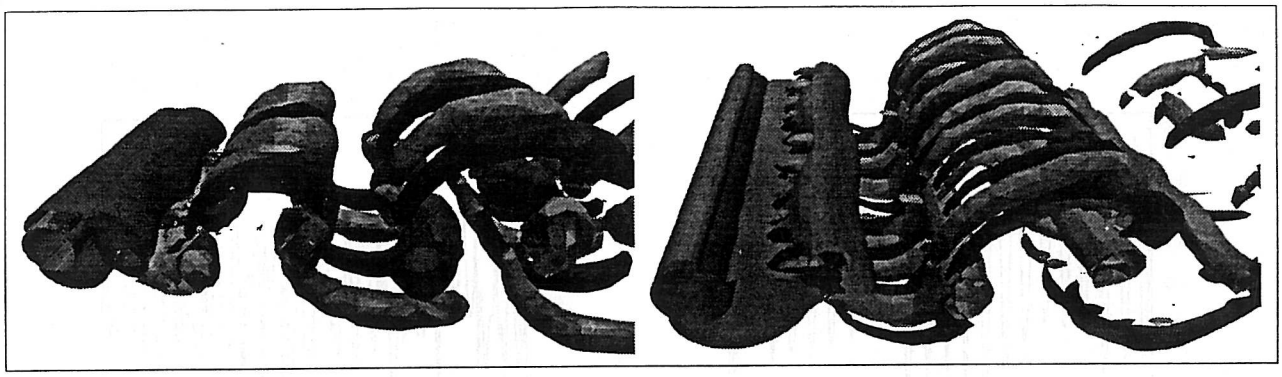

Figure 4: Isosurfaces of pressure ($p = -0.3$) and streamwise vorticity ($\omega_x = \pm 0.3$) at $Re = 250$. The pressure isosurfaces indicate the positions of the Strouhal vortices. The circular cylinder is also shown. Left: Structures after 25 Strouhal periods showing predominantly Mode A shedding. Right: After 40 cycles the spanwise wavelength is much shorter corresponding to Mode B shedding. The cylinder width depicted is $2\pi D$. (The computational domain width for these calculations was πD).

Figure 4 (left) is an isosurface plot visualising the three-dimensional structures in the wake. The figure shows pressure isosurfaces for $p = -0.3$ and streamwise vorticity contours for $\omega_x = \pm 0.3$. The pressure isosurfaces are shown to highlight the predominately two-dimensional Strouhal vortices. The streamwise vorticity isosurfaces are strongly developed at this time ($t = 25$ Strouhal cycles). They connect between the Strouhal vortices. The cylinder section shown is twice the actual computational domain width. The spanwise wavelength is πD which is consistent with the experimentally observed wavelength for Mode A shedding.

After about 40 Strouhal periods from initiation of the three-dimensional disturbance, the three-dimensional structures change in character. Figure 4 (right) shows the iso-surfaces at that time. The spanwise wavelength has been reduced to $\pi/4 \approx 0.8$ diameters. This is more typical of the Mode B shedding observed experimentally.

The simulation was continued for approximately 100 Strouhal cycles and did not show any sign of reaching a steady periodic state. The u and w velocity traces at (1.88,-0.69) are shown in Fig. 5 (The Strouhal period is approximately 10.) There is no obvious indication of period-doubling as was found by Karniadakis and Triantafyllou (1992) and Tomboulides *et al.* (1992) who used a domain width of only half of that used for the present simulations and therefore could not resolve Mode A. Computations using the smaller spanwise domain ($\pi D/2$) do indicate period-doubling at this Reynolds numbers in line with the results from these papers. It is not clear whether the period-doubling exists when the two modes are present together. Indeed, to some extent, at this Reynolds number it appears that the three-dimensional structures seem to alternate between the two different modes. This is consistent with the experimental findings for the transition region between the two shedding modes. In this Reynolds number range, ($230 < Re < 260$), experimental results show two peaks in the frequency spectrum presumably corresponding to the coexistence of the two modes (Williamson 1991a).

Simulation at Other Reynolds Numbers

A computation at $Re = 200$ was carried out starting from a fully-developed three-dimensional

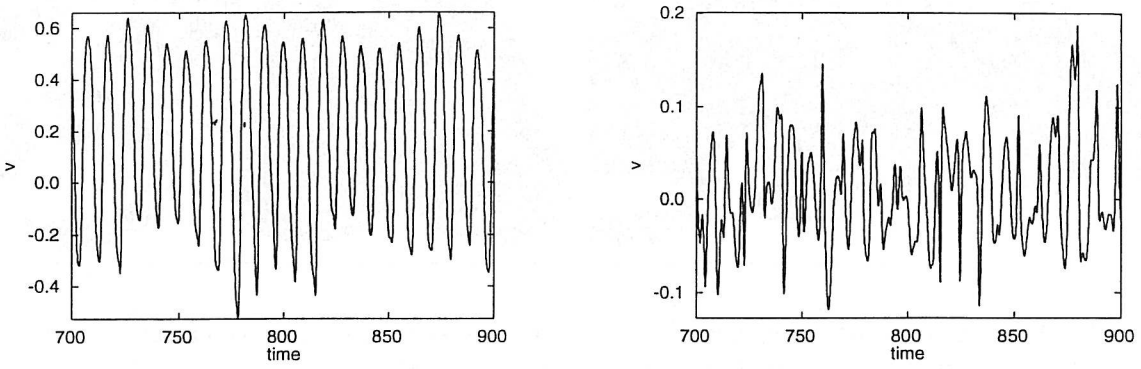

Figure 5: Time evolution of the u (left) and w (right) velocity components at (1.88,-0.69) at $Re = 250$.

velocity field from the simulation at $Re = 250$. After a transition period, the velocity field settles down to periodic state corresponding to Mode A shedding. A simulation at $Re = 210$ gives a similar result but in this case the streamwise vortex structures are stronger.

Effect of Domain Width

In order to test the preferred spanwise wavelength of Mode A, a computation was performed with a domain width of $2\pi D$ and 48 Fourier modes at $Re = 250$. As before, a perturbed two-dimensional velocity field was used to begin the simulation. The results were similar to those found with the narrower domain with the Mode A wavelength again equal to πD.

CONCLUSIONS

Three-dimensional simulations of the flow past an infinite, two-dimensional circular cylinder show features similar to those found experimentally. In particular, the computations predict the two shedding modes which occur for different Reynolds number ranges and give spanwise wavelengths consistent with the experimental values. There are indications that the two modes can coexist for intermediate Reynolds numbers (*i.e.*, $Re = 250$) which is also consistent with experiments.

Computations are currently underway using larger and more refined meshes to try to understand the transition process more fully.

ACKNOWLEDGMENTS

The authors gratefully acknowledge support through a grant from the Australian Research Council.

REFERENCES

Eisenlohr, H. & Eckelmann, H. 1989, 'Vortex splitting and its consequences in the vortex street wake of cylinders at low Reynolds numbers', *Phys. Fluids* **A1**, 189.

Gresho, P. M., Gartling, D. K., Torczynski, J. R., Cliffe, K. A., Winters, K. H., Garratt, T. J., Spence, A., and Goodrich, J. W. 1993, 'Is the steady viscous incompressible two-dimensional flow over a backward-facing step at Re = 800 stable?', *Intl. J. Numer. Meth. Fluids* **17**, 501–541.

Hammache, M. & Gharib, M. 1989, 'A novel method to promote parallel vortex shedding in the wake of a circular cylinder', *Phys. Fluids* A**1**, 1611–1614.

Kaiktsis, L, Karniadakis, G. E. & Orzsag, S. 1991, 'Onset of three-dimensionality, equilibria, and early transition in flow over a backward facing step', *J. Fluid Mech.* **231**, 501–528.

Karniadakis, G. E. & Triantafyllou, G. S. 1992, 'Three-dimensional dynamics and transition to turbulence in the wake of bluff objects', *J. Fluid Mech.* **238**, 1–30.

Karniadakis, G. E. Israeli, M. & Orszag, S. A. 1991, 'High-order splitting methods for the incompressible Navier-Stokes equations', *J. Comp. Phys.* **97**, 414–443.

Norberg, C. 1994, 'An experimental investigation of the flow around a circular cylinder: influence of aspect ratio', *J. Fluid Mech.* **258**, 287.

Roshko, A. 1954, 'On the development of turbulent wakes from vortex streets', *NACA Report 1191.*

Roshko, A. 1955, 'On the wake and drag of bluff bodies' *J. Aero. Sci.* **22**, 124–132.

Tomboulides, A. G., Triantafyllou, G. S. & Karniadakis, G. E. 1992, 'A new mechanism of period doubling in free shear flows', *Phys. Fluids* **4**, 1329–1332.

Williamson, C. H. K. 1988a, 'Defining a universal and continuous Strouhal-Reynolds number relationship for the laminar vortex shedding of a circular cylinder', *Phys. Fluids* **31**, 2742.

Williamson, C. H. K. 1988b, 'The existence of two stages in the transition to three-dimensionality of a cylinder wake', *Phys. Fluids* **31**, 3165.

Williamson, C. H. K. 1991a, '2–D and 3–D aspects of the wake of a cylinder, and their relation to wake computations', *Lectures in Applied Mathematics* **28**, 719–751.

Williamson, C. H. K. 1991b, 'Three-dimensional aspects and transition of the wake of a circular cylinder', *Turbulent Shear Flows 7.* (eds F. Durst, B. E. Launder, W. C. Reynolds, F. W. Schmidt & J. H. Whitelaw). pp. 173–194. Springer-Verlag.